Smart Structures and Systems, *Vol. 18, No. 6 (2016) 1251-1267*
DOI: http://dx.doi.org/10.12989/sss.2016.18.6.1251

Application of simple adaptive control to an MR damper-based control system for seismically excited nonlinear buildings

Majd Javanbakht[a] and Fereidoun Amini*

Department of Civil Engineering, Iran University of Science and Technology, Tehran, Iran

(Received June 23, 2014, Revised March 22, 2016, Accepted April 20, 2016)

Abstract. In this paper, Simple Adaptive Control (SAC) is used to enhance the seismic response of nonlinear tall buildings based on acceleration feedback. Semi-active MR dampers are employed as control actuator due to their reliability and well-known dynamic models. Acceleration feedback is used because of availability, cost-efficiency and reliable measurements of acceleration sensors. However, using acceleration feedback in the control loop causes the structure not to apparently meet some requirements of the SAC algorithm. In addition to defining an appropriate SAC reference model and using inherently stable MR dampers, a modification in the original structure of the SAC is proposed in order to improve its adaptability to the situation in which the plant does not satisfy the algorithm's stability requirements. To investigate the performance of the developed control system, a numerical study is conducted on the benchmark 20-story nonlinear building and the responses of the SAC-controlled structure are compared to an H_2/LQG clipped-optimal controller under the effect of different seismic excitations. As indicated by the results, SAC controller effectively reduces the story drifts and hence the seismically-induced damage throughout the structural members despite its simplicity, independence of structural parameters and while using fewer number of dampers in contrast with the H_2/LQG clipped-optimal controller.

Keywords: seismic control; simple adaptive control; acceleration feedback; MR dampers; nonlinear structures

1. Introduction

Semi-active control systems have been studied both theoretically and experimentally in order to mitigate the deleterious effects of seismic loads on building structures (Casciati, Rodellar *et al*. 2012). The uncertainties in the characteristics of an earthquake excitation and possible changes in the structural properties, cause the passive control systems not to be adaptable to unpredictable conditions. Although active control systems have been widely implemented in practical structures, the need for large external power sources and the probability of structural instability necessitate the designer to seriously consider reliability issues. Semi-active control approach combines the merits of both strategies, namely the reliability of passive systems and the adaptability of active systems while requiring no large power source and not being able to destabilize the controlled structure (Spencer Jr. and Nagarajaiah 2003).

*Corresponding author, Professor, E-mail: famini@iust.ac.ir
[a] Ph.D. Student, Email: javanba@uwindsor.ca

http://www.techno-press.org/?journal=sss&subpage=8 ISSN: 1738-1584 (Print), 1738-1991 (Online)

During the strong ground motions, nonlinear behavior of the structure is initiated by development of plastic hinges throughout the structural members. Since the nonlinear behavior of a structure is totally different from the linear stage, this issue has been considered and incorporated into the benchmark control studies by introducing a finite-element based nonlinear analysis tool in MATLAB/Simulink® environment (Ohtori, Christenson *et al*. 2004). In this benchmark problem, three nonlinear structures (3, 9 and 20-stories) have been defined for designing and evaluating competitive seismic controllers. Several researchers have proposed control systems for the 20-story nonlinear benchmark building. Yoshida and Dyke (2004) have presented a semi-active clipped-optimal H_2/LQG controller based on acceleration feedback to mitigate the seismic response of MR damper-equipped structure. Chen and Chen (2004) have developed a hybrid control algorithm for the structure equipped with piezoelectric friction dampers considering both the stick and sliding phases of dampers. Wongprasert and Symans (2004) have introduced a systematic method for identifying the optimal damper distribution to control the seismic response of the 20-story nonlinear building based on Genetic Algorithm (GA). Ozbulut and Hurlebaus (2012) have investigated the seismic response control of a 20-story nonlinear building equipped with a new Re-centering Variable Friction Device (RVFD) which combines energy dissipation capabilities of a Variable Friction Damper (VFD) with the re-centering ability of Shape Memory Alloy (SMA) wires. The authors designed a fuzzy logic controller to adjust the voltage level of VFDs for favorable performance in an RVFD hybrid application.

Through the last three decades, adaptive controllers have been successfully implemented in complex and large systems such as space structures and flight control systems. As an effort to make these controllers simpler, Sobel, Kaufman *et al*. (1979) introduced Simple Adaptive Control (SAC) method which lies in the category of Direct Model Reference Adaptive Control (DMRAC) scheme. SAC is called "simple" because it does not use observers and identifiers in its feedback loop and the order of reference model is allowed to be smaller than the plant. SAC has been developed through the works of Bar-Kana (1987), Bar-Kana and Guez (1990), Bar-Kana and Kaufman (1993), Bar-Kana (2007), Iwai and Mizumoto (1994), Iwai, Mizumoto *et al*. (2006) and has been used in the structural control efficiently (Hino, Iwai *et al*. 1996, Bitaraf, Hurlebaus *et al*. 2012). Other types of adaptive controllers also have been studied for seismically excited structural systems. Amini and Ghaderi (2013) have presented a robust control scheme to regulate seismic vibrations based on estimating the ground motion and structural damping uncertainties by appropriate adaptive laws and applying a developed adaptive back-stepping control strategy to propose a control law which only depends on feedback measurements of displacement and velocity vectors. Amini and Javanbakht (2014) have used SAC to mitigate the seismic response of linear MR damper-equipped shear buildings based on acceleration feedback where the simulations on both damaged and undamaged structural states show substantial reduction in seismic response.

Extensive studies have been carried out on MR dampers both analytically and experimentally for large-scale as well as model prototypes. Due to highly non-linear characteristic of MR dampers, establishing a dynamic model to reflect their accurate behavior is rather challenging. Spencer, Dyke *et al.* (1997a) have conducted a number of laboratory experiments and proposed a phenomenological model for MR dampers based on Bouc-Wen hysteresis model which has been widely used afterwards. In addition, representative neural network models (Chang and Roschke 1998), fuzzy models (Schurter and Roschke 2000) and polynomial models (Choi, Lee *et al*. 2001) are also developed subsequently. Spencer Jr., Carlson *et al.* (1997b) reported the design of a full-scale 20 ton MR damper and showed the capability of these devices for being used in practical civil engineering structures. In 2001, the first full-scale implementation of MR dampers for civil engineering applications was achieved in Tokyo (Spencer Jr. and Nagarajaiah 2003).

In this study, a modified SAC algorithm is presented for semi-active control of nonlinear 20-story benchmark structure subjected to different earthquake excitations. Acceleration response of the structure is measured via accelerometers and used in the control feedback loop because of the availability, reliability and cost-efficiency of such sensors. MR dampers are selected as the semi-active actuator due to their inherent stability, well-known mathematical models and successful implementation. By using an adaptive controller which is independent of system parameters and by utilizing reliable acceleration sensors and stable MR dampers, this study aims at providing a practical semi-active scheme applicable to complex nonlinear structures. However, using acceleration feedback causes the system not to satisfy some stability conditions of SAC algorithm. This stability issue has been tackled by considering three strategies: a) utilizing inherently stable MR dampers as the semi-active actuator, b) defining an appropriate reference model that is best suited to the nonlinear structure, and c) modifying the original structure of SAC by embedding a PI filter to the algorithm to improve its behavior in the case of acceleration feedback.

To evaluate the efficiency of proposed control system, a numerical study is conducted and the response of SAC-controlled 20-story structure is compared to those of a clipped-optimal H_2/LQG controller. Results indicate an acceptable performance of the SAC controller in reducing the story drifts and induced damage through the structure.

2. Problem formulation

2.1 Simple Adaptive Control (SAC)

As a DMRAC scheme, SAC algorithm was proposed by Sobel, Kaufman *et al.* (1979) as an attempt to make adaptive controllers simpler. This algorithm requires neither full state access nor prior knowledge of plant dynamics, but adaptive stability requires the nonlinear plant to satisfy Almost Strictly Passive (ASP) condition (Kaufman, Bar-Kana *et al.* 1998).

The dynamic nonlinear plant is represented by

$$\dot{x}_p(t)=\mathbf{A_p}(x_p)x_p(t)+\mathbf{B_p}(x_p)u_p(t)+d_p(x_p,t) \tag{1a}$$

$$y_p(t)=\mathbf{C_p}(x_p)x_p(t)+\mathbf{D_p}(x_p)u_p(t)+d_0(x_p,t) \tag{1b}$$

where x_p is the plant state vector, u_p is the control input vector, y_p is the output vector, d_p and d_0 are plant and output disturbances, respectively and the state-dependent matrices $\mathbf{A_p}$, $\mathbf{B_p}$, $\mathbf{C_p}$ and $\mathbf{D_p}$ are uniformly bounded.

For the plant represented by Eq. (1), the ASP condition holds when there exists a positive-definite static feedback gain $\mathrm{K_e}$ (not needed for implementation) such that the resulting closed-loop system is Strictly Passive (SP). In other words, the following Riccati equation must be satisfied

$$\begin{gathered}\dot{\mathbf{P}}(x_p) + \mathbf{P}(x_p)\mathbf{A_{pc}}(x_p) + \mathbf{A}^T_{\mathbf{pc}}(x_p)\mathbf{P}(x_p) + \\ [\mathbf{P}(x_p)\mathbf{B_{pc}}(x_p) - \mathbf{C}^T_{\mathbf{pc}}(x_p)] \cdot [\mathbf{D_{pc}}(x_p) + \mathbf{D}^T_{\mathbf{pc}}(x_p)]^{-1} \cdot [\mathbf{B}^T_{\mathbf{pc}}(x_p)\mathbf{P}(x_p) - \mathbf{C_{pc}}(x_p)] \\ + \mathbf{Q}(x_p) = \mathbf{0}\end{gathered} \tag{2}$$

where $\mathbf{P}(x_p)$ and $\mathbf{Q}(x_p)$ are uniformly bounded positive-definite matrices and

$$\mathbf{A_{pc}}(x_p) = \mathbf{A_p}(x_p) - \mathbf{B_p}(x_p)\mathbf{K_{ec}}(x_p)\mathbf{C_p}(x_p) \tag{3}$$

$$\mathrm{B_{pc}}(x_p) = \mathbf{B_p}(x_p)[\mathbf{I} + \mathbf{K_e}\mathbf{D_p}(x_p)]^{-1} \tag{4}$$

$$\mathbf{C_{pc}}(x_p) = [\mathbf{I} + \mathbf{D_p}(x_p)\mathbf{K_e}]^{-1}\mathbf{C_p}(x_p) \tag{5}$$

$$\mathbf{D_{pc}}(x_p) = [\mathbf{I} + \mathbf{D_p}(x_p)\mathbf{K_e}]^{-1}\mathbf{D_p}(x_p) = \mathbf{D_p}(x_p)[\mathbf{I} + \mathbf{K_e}\mathbf{D_p}(x_p)]^{-1} \tag{6}$$

$$\mathbf{K_{ec}}(x_p) = [\mathbf{I} + \mathbf{K_e}\mathbf{D_p}(x_p)]^{-1}\mathbf{K_e} = \mathbf{K_e}[\mathbf{I} + \mathbf{D_p}(x_p)\mathbf{K_e}]^{-1} \tag{7}$$

For a proper and non-minimum-phase system with $\mathbf{D_p} < 0$, the ASP condition does not apply (Bar-Kana and Guez 1990). Since in the case of acceleration feedback, a negative $\mathbf{D_p}$ appears in the structural state-space model, the plant does not satisfy ASP condition. This issue can be tackled by considering three strategies: a) utilizing inherently stable MR dampers as the semi-active actuator, b) defining an appropriate reference model that is best suited to the nonlinear structure, and c) modifying the original structure of SAC algorithm by embedding a PI filter to the algorithm to improve its behavior in the case of acceleration feedback. These ideas will be discussed in more detail through subsequent sections.

The plant output $y_p(t)$ must track the output of a well-behaved reference model of the form

$$\dot{x}_m(t) = \mathbf{A_m}x_m(t) + \mathbf{B_m}u_m(t) \tag{8a}$$

$$y_m(t) = \mathbf{C_m}x_m(t) + \mathbf{D_m}u_m(t) \tag{8b}$$

where x_m is the model state vector, u_m is the command input vector and y_m is the model output vector. Defining an appropriate reference model that always behaves more appropriate than the plant is an important part of the SAC controller design.

The measured tracking error

$$e_y(t) = y_m(t) - y_p(t) \tag{9}$$

has to be minimized by the adaptive control system. The control command is then calculated by

$$u_p(t) = \mathbf{K}(t)r(t) \tag{10}$$

where

$$\mathbf{K}(t) = \mathbf{K_p}(t) + \mathbf{K_I}(t) \tag{11}$$

$$r(t) = [\, e_y^T(t) \quad x_m^T(t) \quad u_m^T(t)\,]^T \tag{12}$$

The proportional and integral terms of adaptive gain $\mathbf{K}(t)$ are calculated respectively as

$$\mathbf{K_p}(t) = e_y(t) r^T(t) \bar{\mathbf{T}} \tag{13}$$

$$\dot{\mathbf{K}}_\mathbf{I}(t) = e_y(t) r^T(t) \mathbf{T} - \sigma \mathbf{K_I}(t) \tag{14}$$

where the positive definite matrices $\bar{\mathbf{T}}$, $\mathbf{T}$ and the positive value σ are three design parameters of the SAC algorithm and should be tuned by the designer (Bar-Kana and Kaufman 1988). The tuning process of these parameters requires a numerical experiment on the plant. The block diagram of SAC algorithm is shown in Fig. 1.

2.2 Structural, MR damper and sensor dynamics

Since the development and progression of plastic hinges throughout the structural members is inevitable during the strong seismic ground motions, this issue has been included in the benchmark structural control studies by introducing a bilinear hysteresis model which models the behavior of plastic hinges (Fig. 2). The plastic hinges are assumed to occur at the moment resisting beam-column and column-column connections (Ohtori, Christenson *et al*. 2004). A MATLAB® tool has been developed to perform nonlinear time history analysis via Newmark-β integration method (Ohtori and Spencer Jr. 1999).

The nonlinear structural system is governed by the following incremental equation

$$\mathbf{M}\delta\ddot{U} + \mathbf{C}\delta\dot{U} + \mathbf{K}\delta U = -\mathbf{M}\Lambda\delta\ddot{x}_g + \mathbf{\Gamma}\delta f + \delta F_{err} \tag{15}$$

where $\mathbf{M}$, $\mathbf{C}$ and $\mathbf{K}$ are mass, damping and stiffness matrices, respectively; Λ is a column vector of ones and $\delta\ddot{x}_g$ is the ground acceleration increment; $\mathbf{\Gamma}$ is the location matrix of control forces; δf is incremental control force and δF_{err} is the unbalanced force vector resulting from the difference between restoring force evaluated using the hysteresis model and the restoring force assuming constant linear stiffness; and δU is the incremental response vector. Substituting Eq. (15) into the Newmark expressions to solve the incremental equation of motion yields

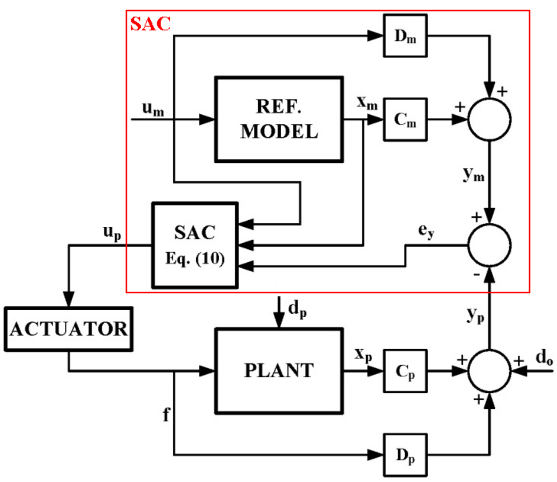

Fig. 1Block diagram of the SAC algorithm

$$\mathbf{T_R}^T\mathbf{K_D}\mathbf{T_R}\delta U_{act} = \mathbf{T_R}^T\delta f_D \tag{16}$$

where δU_{act} is the active node displacement that include all vertical, all rotational and one horizontal DOF per level (assuming the floor slab to be horizontally rigid), $\mathbf{T_R}$ is a transformation matrix for expressing the full response vector in terms of the active degrees of freedom (i.e., $\delta U = \mathbf{T_R}\delta U_{act}$). $\mathbf{K_D}$ and δf_D are given by

$$\mathbf{K_D} = \frac{1}{\beta(\Delta t)^2}\mathbf{M} + \frac{\gamma}{\beta\Delta t}\mathbf{C} + \mathbf{K_t} \tag{17}$$

$$\begin{aligned}\delta f_D = -\mathbf{M}\Lambda\delta\ddot{x}_g + \left(\frac{1}{2\beta}\mathrm{M} + \left(\frac{\gamma}{2\beta} - 1\right)\Delta t\mathbf{C}\right)\ddot{U}_t + \\ \left(\frac{1}{\beta\Delta t}\mathbf{M} + \frac{\gamma}{\beta}\mathbf{C}\right)\dot{U}_t + \mathbf{\Gamma}\delta f + \delta F_{err}\end{aligned} \tag{18}$$

where Δt is the calculation time interval, $\{\ \}_t$ is the response at t, β and γ are the Newmark parameters, $\mathbf{K_t}$ is the tangent stiffness matrix of the structure at time t (calculated based on a concentrated plasticity model) and $\mathbf{C}$ is the damping matrix based on an assumption of Rayleigh damping and is expressed as

$$\mathbf{C} = a_0\mathbf{M} + a_1\mathbf{K} \tag{19}$$

with the coefficients a_0 and a_1 determined from specified damping ratios and natural circular frequencies of i^{th} and j^{th} modes as

$$\frac{1}{2}\begin{bmatrix} 1/\omega_i & \omega_i \\ 1/\omega_j & \omega_j \end{bmatrix}\begin{Bmatrix} a_0 \\ a_1 \end{Bmatrix} = \begin{Bmatrix} \zeta_i \\ \zeta_j \end{Bmatrix} \tag{20}$$

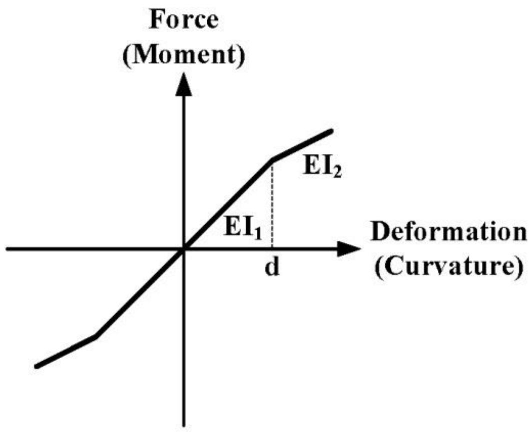

Fig. 2 Bilinear model for the plastic hinges at beam-column connection

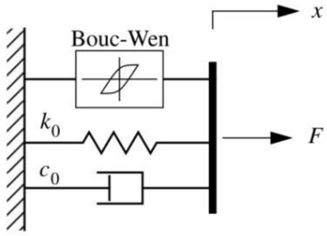

Fig. 3 Bouc-Wen physical model for MR dampers

The phenomenological model of MR damper is introduced by Spencer, Dyke *et al*. (1997a) based on the response of a prototype MR damper through experimental studies. Fig. 3 illustrates the mechanical idealization of MR damper based on a Bouc-Wen hysteresis model which is governed by the following simultaneous nonlinear equations

$$f = \alpha z + c_0 \dot{x} \tag{21}$$

$$\dot{z} = -\gamma |\dot{x}| z |z|^{n-1} - \beta (\dot{x}) |z|^n + A\dot{x} \tag{22}$$

where f and $\dot{x}$ are the damper force and velocity, respectively; c_0 is the observed viscous damping at large velocities; z is an evolutionary variable that describes the hysteretic characteristic of MR damper; γ and β affect the shape and A affects the slope of hysteresis loop, while n governs the smoothness of linear to non-linear transition.

The voltage-dependent model parameters are given by the following equations

$$\alpha = \alpha_a + \alpha_b u \tag{23}$$

$$c_0 = c_{0a} + c_{0b} u \tag{24}$$

$$\dot{u} = -\eta (u - v) \tag{25}$$

where Eq. (25) is a first order filter to account for the dynamics of rheological equilibrium of MR fluid and v is the command voltage sent to damper's current driver. A total number of 9 parameters for a prototype MR damper are given in Table 1. The saturation voltage for this damper is reported as 10 V.

Table 1 Bouc-Wen Parameters for the 1000 kN MR damper (Jung, Spencer *et al*. 2003)

Parameter	Value	Parameter	Value
c_{0a}	105.4 kN.sec/m	A	2074.5
c_{0b}	131.6 kN.sec/m.V	n	2
α_a	26.0 kN/m	γ	141.0 m^{-n}
α_b	29.1 kN/m.V	β	141.0 m^{-n}
η	100 sec^{-1}	V_{max}	10 V

One of the challenges associated with MR damper implementation is determining the appropriate command voltage in order to translate the required control force into applied damper force. Several approaches have been introduced in the literature to model the MR damper inverse behavior (Vadtala, Soni *et al*. 2013, Choi, Cho *et al*. 2004, Zhang, Huang *et al*. 2011, Mohajer Rahbari, Farahmand Azar *et al*. 2013). A simplified mathematical model for the MR damper inverse dynamics is used in this study for converting control force to MR damper voltage and is represented as (Tse and Chang 2004)

$$u=\frac{f-c_{0a}\dot{x}-\alpha_a z}{c_{0b}\dot{x}+\alpha_b z} \tag{26}$$

$$z \approx sign(\dot{x})\left(\frac{A}{\gamma+\beta}\right)^{1/n} \tag{27}$$

$$v = u + \frac{\dot{u}}{\eta} \tag{28}$$

Acceleration feedback structural control has been studied experimentally and showed efficiency because of reliability, availability and low cost of accelerometers (Dyke, Spencer *et al*. 1996, Yi, Dyke *et al*. 2001). The acceleration sensors in this study are assumed to have a constant magnitude and phase. The sensor output is governed by the following equation

$$y_s=\mathbf{D_s} y_p + v \tag{29}$$

where y_s and y_p are the sensor and structure output vector, respectively; $\mathbf{D_s}$ is the sensor sensitivity equal to $\mathbf{D_s} = (10/9.81)\mathbf{I}_{m\times m}$ V/m/sec^2 where m is the number of outputs and v is the measurement noise which contains an RMS noise of 0.03 V. The measurement noise is modeled as Gaussian rectangular pulses with a width of 0.01 sec.

3. Numerical study

To evaluate the efficiency and performance of the semi-active adaptive control system, the 20-story nonlinear benchmark structure is studied through numerical simulations. This 20-story steel moment-resisting frame is equipped with MR damper devices in various floors and is subjected to four different earthquake records while the acceleration response of the structure is measured via modeled accelerometers. Fig. 4 illustrates some details of the studied 20-story steel moment-resisting frame. Nonlinear behavior is considered in the structure by defining flexural plastic hinges at beam-column connections. Column splices are not separately modeled and average properties are assigned to the spliced columns. More information about this structure can be found in Ohtori, Christenson *et al.* (2004). A simple adaptive controller is designed to mitigate the seismic response and subsequent damage in the building based on acceleration feedback. The performance of SAC controller is compared to an H_2/LQG clipped-optimal controller by assessing different evaluation criteria specifically defined in benchmark control study. The considered clipped-optimal controller uses the same type of actuator and feedback and therefore is suitable for comparison purposes. The following sections describe the details regarding controller design and numerical analysis.

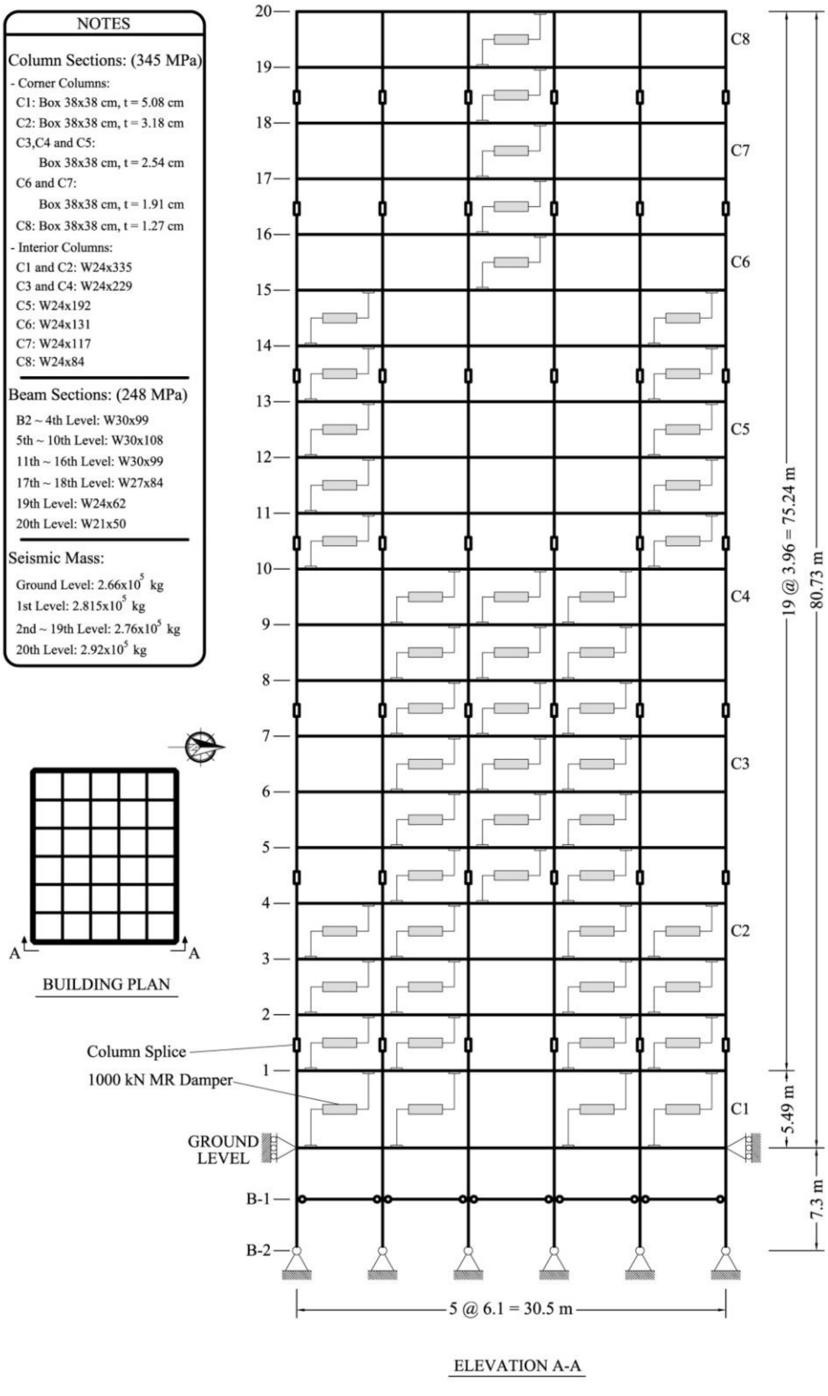

Fig. 4 benchmark 20-story nonlinear moment-resisting steel frame (N-S direction)

3.1 Controller design

Requiring no prior access to plant parameters and having simple and fast structure, Simple adaptive controllers have been successfully implemented in complex and large systems. In the case of nonlinear systems, the adaptive stability of controller requires the plant to satisfy ASP. For a proper non minimum-phase system with $\mathbf{D_p} < 0$, however, this condition does not hold (Bar-Kana and Guez 1990). Since in the case of acceleration feedback, a negative $\mathbf{D_p}$ appears in the structural state-space model (due to interaction between the applied control force and the measured acceleration responses), the plant does not satisfy ASP condition. In order to tackle this issue, three strategies have been considered in this study. First, the inherently stable MR dampers are utilized as semi-active actuators to prevent structural instability due to unbalanced actuator loads.

Second, an appropriate reference model is defined. Reference model is an important part of SAC algorithm and defines an appropriate behavior to be continuously tracked by the plant. In this study, the reference model is defined based on parameter studies as

$$\mathbf{A_m} = -1 \times \mathbf{I}_{20}; \mathbf{B_m} = \mathbf{0}_{20\times1}; \mathbf{C_m} = \mathbf{I}_{20}; \mathbf{D_m} = \mathbf{0}_{20\times1} \tag{30}$$

where the model command input u_m is a unit step function and initial condition is selected as $x_m(0) = 0.1 \times \mathbf{I}_{20\times1}$. Reference model output is shown in Fig. 5. The reference model starts at $t = 0$ sec whenever an earthquake occurrence is detected.

Finally, to improve the algorithm performance for a non-ASP plant, a slight modification in the original structure of SAC has been applied. Since the acceleration feedback causes stability issues in the adaptive controller by contravening the ASP condition (since a negative $\mathbf{D_p}$ appears in the structural state-space model), the plant output is passed through a PI controller before being compared to the model output. The PI controller is defined as

$$G_{PI}(s) = k_p + \frac{k_i}{s} \tag{31}$$

where the proportional and integral gains in this study are selected as $k_p = 0.1$ and $k_i = 0.6$ to obtain the best results. The integral gain produces a velocity set-point which is more stable to be compared with reference model output. The block diagram of embedded PI controller is shown in Fig. 6.

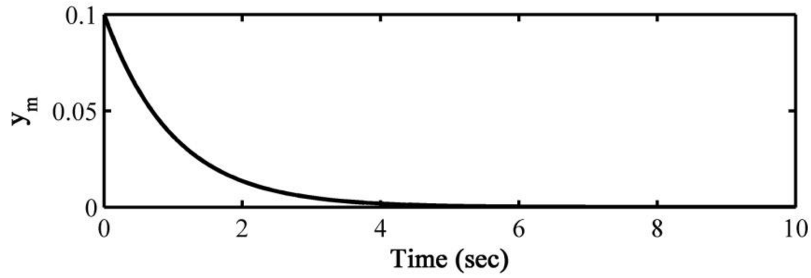

Fig. 5 Reference model output in the SAC algorithm

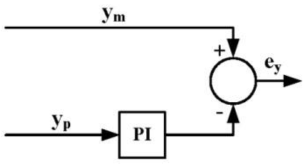

Fig. 6 Block diagram of embedded PI controller in the SAC algorithm

The SAC algorithm parameters are then tuned through several iterations to obtain the best results as $\overline{\mathbf{T}} = 10^6 \times \mathbf{I}_{41}, \mathbf{T} = 10 \times \mathbf{I}_{41}$ and $\sigma = 0.01$. The generated control command by SAC algorithm is converted to MR damper voltage using the inverse model described in Section 2.2.

A clipped-optimal H_2/LQG controller has been designed for the benchmark problem in the work of Yoshida and Dyke (2004). A modified clipping algorithm is introduced to translate control force into MR damper voltage and acceleration response of 5 stories (i.e., story 4, 8, 12, 16 and 20) is used in the feedback loop. Also the weighting matrices $\mathbf{Q}$ and $\mathbf{P}$ are selected through parameter studies as $\mathbf{Q} = 10^{13} \times \mathbf{I}_{20}$ and $\mathbf{P} = diag(\, n_1^2 \quad n_2^2 \quad \ldots \quad n_{20}^2 \,)$ where n_i is the number of MR dampers in the i^{th} story. The number of 1000 kN devices on each story (totally 65 MR dampers) are determined as four devices on the first eight stories, three devices on the next nine stories and two devices on the top two stories. The results of this study (denoted as MCO) are adopted for comparison purposes in the next section.

3.2 Numerical simulation and results

The MR damper equipped 20-story nonlinear building is subjected to four earthquake records as given in Table 2. Various PGA levels of each earthquake are considered, namely, 0.5, 1.0 and 1.5 times the magnitude of El Centro and Hachinohe, and 0.5 and 1.0 times the magnitude of Northridge and Kobe (totally 10 simulation cases).

The required number of 1000 kN MR dampers on each story is determined based on the demand of Northridge (1.0) earthquake. A total number of 49 devices are used; 4 devices on first four stories, 3 devices on next six stories, 2 devices on next five levels and 1 device on the upper five stories. The control force on each story is equally distributed between the MR dampers placed on that story. Since every damper is rigidly connected between two successive levels, the total required control force for each level is transformed to total required device force by the following

$$\{f(t)\}_{20\times 1} = \begin{bmatrix} 1 & -1 & 0 & \cdots & 0 \\ 0 & 1 & -1 & \cdots & 0 \\ 0 & 0 & 1 & \cdots & 0 \\ \vdots & \vdots & \vdots & \ddots & \vdots \\ 0 & 0 & 0 & \cdots & 1 \end{bmatrix}_{20\times 20}^{-1} \{u_p(t)\}_{20\times 1} \tag{32}$$

where $f(t)_i$ is the total damper force in i^{th} story (devices connected between $i-1$ and i stories) and $u_p(t)_i$ is the total control force in that story.

Table 2 Summary of earthquake records used in the simulations

Earthquake name and date	Station and component	PGA $(\mathrm{m/sec}^2)$
Imperial Valley (1940)	El Centro (N-S)	3.417
Takochi-oki (1968)	Hachinohe (N-S)	2.250
Northridge (1994)	Sylmar County (N-S)	8.268
Kobe (1995)	KJMA (N-S)	8.178

The simulation is performed at a constant time step of 0.001 sec and the parameters of Newmark-β method are set as $\beta = 1/4$ and $\gamma = 1/2$ to stabilize the calculations. Also the modal damping coefficients of Rayleigh damping are set as $\zeta_1 = \zeta_5 = 0.02$. The absolute acceleration of each story is measured using accelerometers and used in control feedback loop while the acceleration sensor is modeled based on Eq. (29). The first 10 natural circular frequencies of the 20-story benchmark structure are 1.642, 4.729, 8.162, 11.481, 15.068, 15.341, 18.363, 18.885, 22.818 and 23.143 rad/sec.

The reference model is the innovative part of the SAC algorithm which is defined by the designer to obtain desired control objectives. In this study, in addition to modifying the algorithm's structure, the reference model is designed and tuned to enhance the algorithm performance which is affected by using acceleration feedback in the control loop.

Fig. 7 illustrates the peak story drift ratio and peak acceleration of each floor of the uncontrolled and controlled structure under the effect of four full scale earthquakes. The results of a sub-optimal controller reported in the work of Yoshida and Dyke (2004), denoted as modified clipped optimal (MCO), are also adopted. It can be seen that the SAC algorithm has reduced story drifts effectively in all earthquake cases (especially far-field records: El Centro and Hachinohe) despite an increase in the acceleration levels. Although mitigating the floor accelerations is essential for protecting vibration-sensitive devices and easement of occupants, the damage of a tall building is mainly caused by floor relative displacements. Hence the control objective here is to mitigate structural damage and parameters have been tuned to reduce primarily the story drifts.

In order to compare the performance of competitive control approaches, several evaluation criteria have been introduced in benchmark control studies. Table 3 summarizes the criteria utilized in this study. The permanent story drift criterion (J_{11}) has been proposed by Yoshida and Dyke (2004) in addition to the conventional benchmark criteria. Sufficient simulation time must be considered to allow the response of the structure to attenuate. For the El Centro, Hachinohe and Northridge a duration of 100 sec and for the Kobe earthquake a duration of 180 sec has been used in the simulations.

The ductility and dissipated energy are specific to nonlinear structures to assess the building damage during the seismic excitation. The seventh to tenth criteria are defined to address this issue. In J_7, the ϕ_j is the ratio of curvature at the ends of j^{th} member to the yield curvature of that end. Also In J_8, E_j is the ratio of dissipated energy at the ends of j^{th} member to the dissipated energy at yield of that end. These damage-related parameters are calculated by the nonlinear structural analysis tool during the simulation.

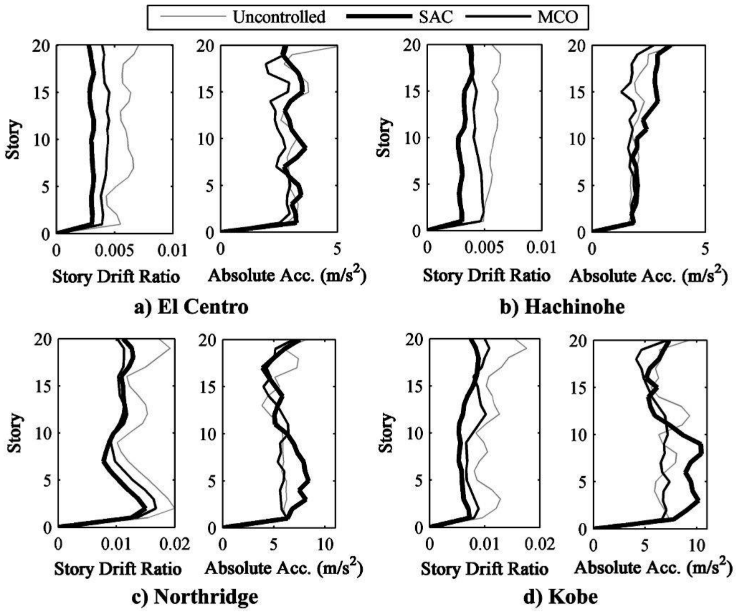

Fig. 7 Peak response of the structure floors subjected to different earthquakes (PGA scale=1)

Table 3 Summary of the evaluation criteria

Peak Story Drift	Peak Level Acceleration	Peak Base Shear
$J_1 = \dfrac{\max\lvert d_i(t)\rvert}{d^{\max}}$	$J_2 = \dfrac{\max\lvert \ddot{x}_i(t)\rvert}{\ddot{x}^{\max}}$	$J_3 = \dfrac{\max\left\lvert \sum_i m_i \ddot{x}_i(t)\right\rvert}{F_b^{\max}}$
Normed Story Drift	Normed Level Acceleration	Normed Base Shear
$J_4 = \dfrac{\max\lVert d_i(t)\rVert}{\lVert d^{\max}\rVert}$	$J_5 = \dfrac{\max\lVert \ddot{x}_i(t)\rVert}{\lVert \ddot{x}^{\max}\rVert}$	$J_6 = \dfrac{\max\left\lVert \sum_i m_i \ddot{x}_i(t)\right\rVert}{\lVert F_b^{\max}\rVert}$
Ductility	Dissipated Energy	Plastic Connections
$J_7 = \dfrac{\max\lvert \phi_j(t)\rvert}{\phi^{\max}}$	$J_8 = \dfrac{\max\lvert E_j(t)\rvert}{E^{\max}}$	$J_9 = \dfrac{N_d^C}{N_d}$
Normed Ductility	Permanent Story Drift	Control Force
$J_{10} = \dfrac{\max\lVert \phi_j(t)\rVert}{\lVert \phi^{\max}\rVert}$	$J_{11} = \dfrac{\max\lvert d_{pi}(t)\rvert}{d_p^{\max}}$	$J_{12} = \dfrac{\max\lvert f_i(t)\rvert}{W}$

Fig. 8 illustrate the calculated evaluation criteria for different earthquake cases and for the SAC, Passive-On (P-On) and MCO controllers. Passive-On is an operational passive case in which the command voltage of MR damper is constantly held at the damper's saturation level (i.e., $v = V_{max}$). Although the SAC utilizes fewer number of MR dampers in contrast with MCO, and despite its simple structure and having no access to structural parameters, it shows acceptable performance in reducing the story drifts up to 50% of uncontrolled structure in almost all excitation cases (J_1). The SAC increases the peak level accelerations but in almost all cases, the maximum acceleration of controlled structure does not surpass the uncontrolled one (J_2).

The normed criteria are considered to assess the controllers from the aspects that may not be provided by peak-related criteria. The performance of SAC controller in level acceleration reduction is improved as is suggested by J_5 and J_6. The next five criteria reflect the damage in the structure. The SAC shows efficiency in reducing the connection curvatures and the number of plastic hinges. In almost all cases except NO(1), SAC prevents the generation of plastic hinges in the structure which is a significant result (J_9).

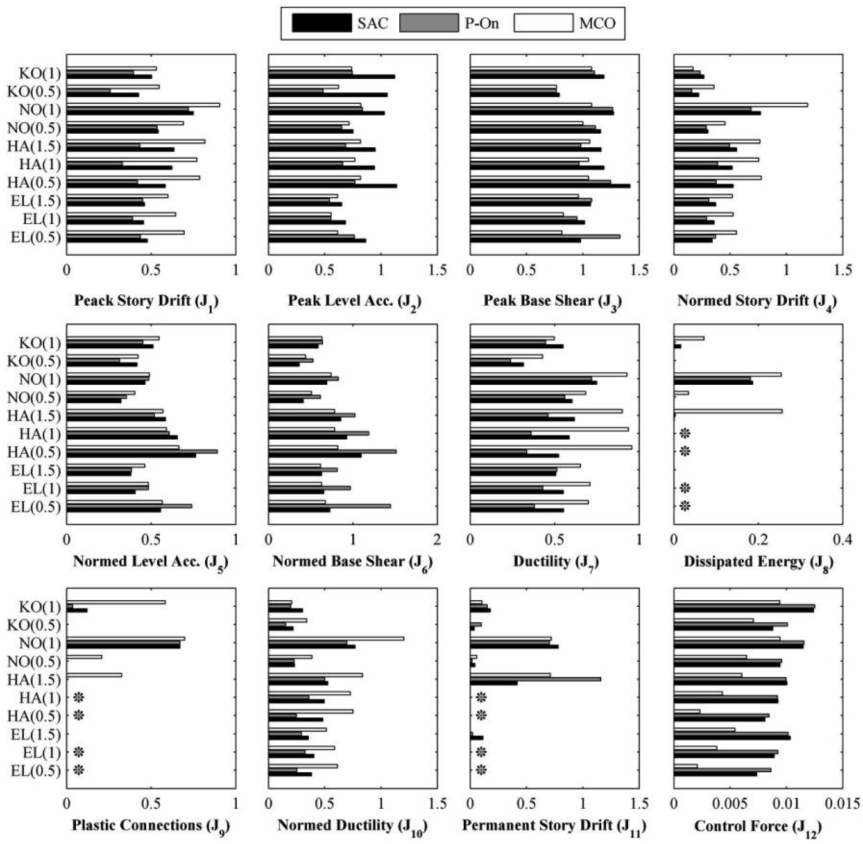

Fig. 8 Evaluation criteria comparison for different controllers (∗ : structure does not yield)

The fewer number of MR dampers especially in the upper stories, causes the maximum control forces of SAC to surpass those of the MCO algorithm, as is shown by last criterion, J_{12}. The larger control force produces higher acceleration levels at the stories, which may not be desirable based on the control objective. However, reducing the number of actuators is always cost-effective and advantageous.

In order to more precisely compare the performance of SAC and MCO algorithms, the structure equipped with the same MR dampers configuration as in the work of Yoshida and Dyke (2004) is again studied for SAC algorithm. Fig. 9 shows the time history of absolute acceleration and inter-story drift of the 20^{th} story of the strcture subjected to the full-scale El Centro and Kobe earthquakes. The number of 1000 kN devices on each story (totally 65 MR dampers) are selected as four devices on the first eight stories, three devices on the next nine stories and two devices on the top two stories. As is shown, the SAC controller has more effectively reduced the drift response for both earthquakes while no significant increase can be observed in the story acceleration response in contrast with the MCO, especially for the Kobe ground motion.

The SAC algorithm generally shows acceptable performance compared to an H_2/LQG clipped-optimal controller. It has been used to mitigate the seismic response of a complicated nonlinear tall building assuming no access to the dynamic parameters of the structure. The stability of the controller is guaranteed whenever the controlled system meets the ASP condition. However, using acceleration feedback makes it difficult to meet the condition directly. Utilizing the stable MR dampers and modifying the algorithm has made it possible to successfully implement the method.

4. Conclusions

In this study, a simple adaptive controller is used to enhance the seismic response of 20-story nonlinear benchmark building based on acceleration feedback. Semi-active MR dampers are employed to improve the applicability and reliability of proposed control system. The SAC needs no prior knowledge on plant parameters and its simple structure and few design parameters, make it a candidate controller for complex and large systems which has been successfully implemented in the last two decades. Using acceleration feedback causes some difficulties in satisfying SAC required stability conditions. However, by utilizing inherently stable MR damper devices, defining an appropriate reference model which fits into the control objectives and by embedding a PI filter into the SAC original structure, this issue has been tackled. The results of the numerical simulation indicate the efficiency of SAC in reducing the peak story drifts as well as the number of plastic hinges compared to a clipped-optimal H_2/LQG controller. Despite using fewer number of MR dampers in contrast with the sub-optimal controller, the SAC has reduced the maximum story drifts more effectively. By using the same number of MR dampers, the SAC shows a more efficient performance comparing to the MCO as is observed in the time history responses. The larger control forces affect the SAC algorithm performance in reducing story accelerations which may not be considered as control objective in the case of tall buildings. The performance of the proposed semi-active adaptive control scheme is acceptable regarding the practical aspects inherent in such a system, especially the algorithm’s reliance on only measured outputs.

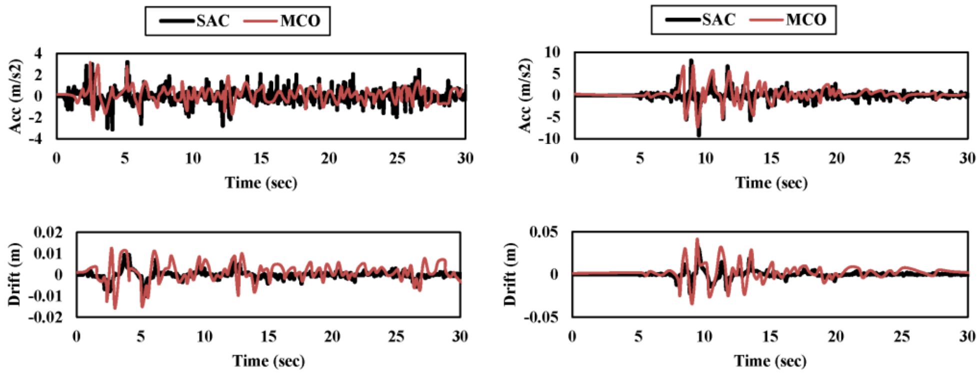

(a) El Centro (b) Kobe

Fig. 9 Comparison of control algorithm performance for the structure equipped with identical MR damper configuration

References

Amini, F. and Ghaderi, P. (2013), "Seismic motion control of structures: A developed adaptive backstepping approach", *Comput. Struct.*, **114-115,** 18-25.

Amini, F. and Javanbakht, M. (2014), "Simple adaptive control of seismically excited structures with MR dampers", *Struct.Eng. Mech.*, **52**(2), 275-290.

Bar-Kana, I. (1987), "Parallel feedforward and simplified adaptive control", *Int. J. Adaptive Control Signal Pr.*, **1**(2)**,** 95-109.

Bar-Kana, I. (2007), "Adaptive model tracking with mitigated passivity conditions", *Proceedings of the 9th Workshop on Adaptation and Learning in Control and Signal Processing (ALCOSP'07)*, St. Petersburg, Russia, August.

Bar-Kana, I. and Guez, A. (1990), "Simple adaptive control for a class of non-linear systems with application to robotics", *Int. J. Control*, **52**(1), 77-99.

Bar-Kana, I. and Kaufman, H. (1988), "Simple adaptive control of uncertain systems", *Int. J. Adaptive Control Signal Pr.*, **2**(2)**,** 133-143.

Bar-Kana, I. and Kaufman, H. (1993), "Simple adaptive control of large flexible space structures", *IEEE T. Aerospace Electronic Syst.*, **29**(4)**,** 1137-1149.

Bitaraf, M., Hurlebaus, S. and Barroso, L.R. (2012), "Active and semi-active adaptive control for undamaged and damaged building structures under seismic load", *Comput. - Aided Civil Infrastruct. E.*, **27**(1), 48-64.

Casciati, F., Rodellar, J. and Yildirim, U. (2012), "Active and semi-active control of structures - theory and applications: A review of recent advances", *J. Intel. Mat. Syst. Str*., **23**(11)**,** 1181-1195.

Chang, C. and Roschke, P. (1998), "Neural network modeling of a magnetorheological damper", *J. Intel. Mat. Syst. Str.*, **9**(9), 755-764.

Chen, G. and Chen, C. (2004), "Semiactive control of the 20-story benchmark building with piezoelectric friction dampers", *J. Eng. Mech.- ASCE*, **130**, 393-400.

Choi, K.M., Cho, S.W., Jung, H.J. and Lee, I.W. (2004), "Semi-active fuzzy control for seismic response reduction using magnetorheological dampers", *Earthq. Eng. Struct. D.*, **33**(6), 723-736.

Choi, S., Lee, S. and Park, Y. (2001), "A hysteresis model for the field-dependent damping force of a magnetorheological damper", *J. Sound Vib.*, **245** (2), 375-383.

Dyke, S., Spencer Jr., B.F., Sain, M. and Carlson, J. (1996), "Experimental verification of semi-active structural control strategies using acceleration feedback", *Proceedings of the 3rd International Conference*

on Motion and Vibration Control, Chiba, JAPAN, September.
Hino, M., Iwai, Z., Mizumoto, I. and Kohzawa, R. (1996), "Active vibration control of a multi-degree-of-freedom structure by the use of robust decentralized simple adaptive control", *Proceedings of the 1996 IEEE International Conference on Control Application*, Dearborn, USA, September.
Iwai, Z. and Mizumoto, I. (1994), "Realization of simple adaptive control by using parallel feedforward compensator", *Int. J. Control*, **59**(6), 1543-1565.
Iwai, Z., Mizumoto, I. and Nakashima, Y. (2006), "Multivariable stable PID controller design with parallel feedforward compensator", *Proceedings of the SICE-ICASE, 2006. International Joint Conference*, Busan, October.
Jung, H.J., Spencer Jr., B.F. and Lee, I.W. (2003), "Control of seismically excited cable-stayed bridge employing magnetorheological fluid dampers", *J. Struct. Eng. - ASCE*, **129**(7), 873-883.
Kaufman, H., Bar-Kana, I. and Sobel, K. (1998), *Direct Adaptive Control Algorithms: Theory and Applications*, Springer, New York, NY, USA.
Mohajer Rahbari, N., Farahmand Azar, B., Talatahari, S. and Safari, H. (2013), "Semi-active direct control method for seismic alleviation of structures using MR dampers", *Struct. Control Health Monit.*, **20**(6), 1021-1042.
Ohtori, Y. and Spencer Jr., B.F. (1999), "A MATLAB-based tool for nonlinear structural analysis", *Proceedings of the 13th ASCE Engineering Mechanics Division Specialty Conference*, Baltimore, June.
Ohtori, Y., Christenson, R., Spencer Jr., B.F. and Dyke, S. (2004), "Benchmark control problems for seismically excited nonlinear buildings", *J. Eng. Mech. - ASCE*, **130**(4), 366-385.
Ozbulut, O. E. and Hurlebaus, S. (2012), "Application of an SMA-based hybrid control device to 20-story nonlinear benchmark building", *Earthq. Eng. Struct. D.*, **41**(13), 1831-1843.
Schurter, K.C. and Roschke, P.N. (2000), "Fuzzy modeling of a magnetorheological damper using ANFIS", *Proceedings of the 9th IEEE International Conference on Fuzzy Systems*.
Sobel, K., Kaufman, H. and Mabius, L. (1979), "Model reference output adaptive control systems without parameter identification", *Proceedings of the 18th IEEE Conference on Decision and Control including the Symposium on Adaptive Processes.*
Spencer Jr., B.F. and Nagarajaiah, S. (2003), "State of the art of structural control", *J. Struct. Eng. - ASCE*, **129**(7), 845-856.
Spencer Jr., B.F., Carlson, J.D., Sain, M. and Yang, G. (1997b), "On the current status of magnetorheological dampers: Seismic protection of full-scale structures", *Proceedings of the American Control Conference*.
Spencer, B., Dyke, S., Sain, M. and Carlson, J. (1997a), "Phenomenological model for magnetorheological dampers", *J. Eng. Mech. - ASCE*, **123**(3), 230-238.
Tse, T. and Chang, C. (2004), "Shear-mode rotary magnetorheological damper for small-scale structural control experiments", *J. Struct. Eng. - ASCE*, **130**(6), 904-911.
Vadtala, I.H., Soni, D.P. and Panchal, D.G. (2013), "Semi-active control of a benchmark building using neuro-inverse dynamics of MR damper", *Procedia Eng.*, **51**, 45-54.
Wongprasert, N. and Symans, M. (2004), "Application of a genetic algorithm for optimal damper distribution within the nonlinear seismic benchmark building", *J. Eng. Mech. - ASCE*. **130**, 401–406.
Yi, F., Dyke, S.J., Caicedo, J.M. and Carlson, J.D. (2001), "Experimental verification of multiinput seismic control strategies for smart dampers", *J. Eng. Mech. - ASCE*, **127**(11), 1152-1164.
Yoshida, O. and Dyke, S.J. (2004), "Seismic control of a nonlinear benchmark building using smart dampers", *J. Eng. Mech. - ASCE*, **130**(4), 386-392.
Zhang, Z.Y., Huang, C.X., Liu, X. and Wang, X.H. (2011), "A Novel Simplified and High-Precision Inverse Dynamics Model for Magneto-Rheological Damper", *Appl. Mech. Mater.*, **117-119**, 273-278.

CY